

www.jpis.az

On the issue of color interpretation in image processing by an onboard vision system

Vagif Aliyev

Institute of Control Systems, 68, B. Vahabzade str., AZ1141, Baku, Azerbaijan

vagifaliyev@hotmail.com

orcid.org/0009-0000-5073-9573

ARTICLE INFO

<https://doi.org/10.25045/jpis.v17.i1.10>

Article history:

Received 16 September 2025

Received in revised form

18 November 2025

Accepted 19 January 2026

Keywords:

Onboard vision system

Image of the Earth's surface

RGB model

Image recognition

Signal processing

Recognition method

Pairwise comparison of signals

ABSTRACT

Color sensing has become an essential technology in computer vision, with significant applications in agriculture, manufacturing, healthcare, and automation. It enables machines to accurately detect, distinguish, and interpret colors, supporting critical tasks such as object tracking, quality control, and informed decision-making. While advanced artificial intelligence tools are increasingly integrated into daily life, color recognition remains a simple, reliable, and efficient solution, especially in controlled environments where precision and speed are paramount. A color model, or color space, provides a structured numerical framework for representing colors, ensuring consistent interpretation across different digital devices and imaging systems. Among the available models is the most commonly used due to its straightforward implementation and broad compatibility. This article reviews widely adopted methods for color space analysis and proposes a novel approach to color interpretation. The proposed method combines low computational complexity, high processing speed, ease of implementation, and robustness to variations in object orientation. These features make it particularly well-suited for onboard vision systems and practical real-world applications, enhancing the efficiency and reliability of color-based image processing.

1. Introduction

Color recognition uses the Red, Green, And Blue (RGB) model to automate computer vision decisions. Computer vision is an Artificial Intelligence (AI) tool that allows devices to analyze and understand visual data. A key aspect of this branch is color recognition, which enables devices to identify and distinguish objects based on color. By analyzing pixel values in different color spaces, color recognition is actively used in the onboard vision systems of quadcopters that track the Earth's landscapes during autonomous piloting. Color detection focuses on identifying specific colors in an image, while object detection involves recognizing and classifying objects regardless of their color. In the self-driving quadcopter scenario, color detection identifies the green color of vegetation, while object detection

identifies the landscape itself, helping the quadcopter maneuver when disconnected from Global Positioning System (GPS) signals.

RGB models are widely used in digital image processing. These models create different colors by combining different levels of red, green, and blue light. Although RGB is simple and popular, it does have some limitations. Colors don't always appear the same to the human eye because RGB does not uniformly correspond to how we perceive color differences. It's also affected by lighting conditions, meaning colors can look different depending on brightness and environment. There are three commonly used RGB models: Lightness, Average and Luminosity (John, 2025). The article discusses a new approach to interpreting color in shades of gray. The adequacy of this approach is assessed in

comparison with the listed RGB models based on a computational experiment.

2. Related work

In research conducted several decades ago, the so-called color codebook with a limited number of colors (usually 100-200) was used to replace the color gamut and obtain a high-quality reconstructed color image (Wang, 1992). As a result, color images were displayed on less expensive devices while maintaining high quality and occupying less memory. However, the color codebook usually has a random structure, and the encoded image, called an index image, has no structure. Therefore, this prevented the use of the codebook representation of the color image in further image processing.

Many decades ago, studies were conducted on invariant spectral features that were suitable for identifying color in the range of existing lighting (Berry, 1987). The histograms of the selected recognition features created at that time were then used to form a spectral signature of objects of similar structure, which, in turn, ensured more accurate recognition. The issue of taking into account the color range in images has always been relevant in recognition theory. The paper gave an affirmative answer, which shed light on the role of chromatic information for recognizing real images (Oliva and Schyns, 1996).

Most color images obtained by various digital cameras do not provide a quality image corresponding to human perception. The (Muttayane, 2006) discusses a method for color correction of color images obtained by Waikato Image Ranger using three different light sources. This article notes that the color image obtained by Waikato Image Ranger is not of high quality, since the light sources used do not correspond to standard RGB sources. The spectral power distribution values of the light sources were measured using a spectroradiometer.

In (Afifi et al, 2019), a comprehensive review of color balance and illumination estimation methods discusses both classical and modern algorithms for compensating color distortions in computer vision systems. It has been established that multispectral data allows for a more sophisticated approach to color recognition than RGB. This requires more complex methods of image acquisition, but well-proven pattern recognition algorithms can be used. Thus, (Batchelor, 2012) proposes image segmentation methods that can be used to isolate areas by "standard" colors ("red", "yellow", "green", etc.) and colors specific to a particular situation. In particular,

(Haindl and Stanislav, 2005) presents a fast and robust method for multispectral texture segmentation with an unknown number of classes, where individual decorrelated monospectral texture factors are represented by four local autoregressive random field models, recursively estimated for each pixel and for each spectral band.

Solutions to many image processing problems involve detection of so-called key points. While there are many approaches using gray levels, color and hyperspectral ones are rare. Thus, (Chatoux et al., 2020) proposes a universal method for detecting key points for color, multispectral and hyperspectral images. A new synthetic database has been created to compare different approaches to detecting key points. The proposed method improves the quality of recognition with increasing image complexity.

The K-nearest neighbors (KNN) method is widely used in neural network modeling and machine learning to classify various objects. In particular, it is successfully applied in recognition using neural networks and digital image processing. In the (Bayraktar et al., 2020) the KNN classifier is used to distinguish 12 different colors: black, blue, brown, forest, green, dark blue, orange, pink, red, purple, white and yellow. By extracting features from the color histogram, the selected image processing method identifies features that distinguish these colors. These features increase the efficiency of the KNN classifier. Many image processing algorithms employ derivatives, which can achieve superior results in applications such as edge detection. In particular, the paper (Henriques et al., 2021), which focuses on grayscale images, implements algorithms for six fractional detectors for color images and illustrates their effectiveness. It discusses the Sobel, CRONE, Roberts, Canny, Laplace-Gauss, and fractional derivative algorithms. Based on the prerequisites of the analysis of existing methods for determining the color tones of images, the importance and relevance of developing an information processing system and software for determining the dominant color tones of images becomes obvious. The (Gijssen et al, 21012) demonstrates that the choice of color space significantly affects the detectability and discriminability of colored objects.

The study (Karaimer and Brown, 2018) presents techniques for extracting color information in various color spaces (RGB, HSV, CIELAB) for machine vision and image analysis tasks. According to (Barron, 2015), the approach based on image processing algorithms for computationally constrained platforms demonstrates robustness to noise and illumination changes in color interpretation tasks.

3. Material and methods

Unlike a human, the quadcopter's vision system "does not see colors" – it processes them as data, converting shades and colors into numerical values. The image of the Earth's landscape i_{01} , recorded by the onboard camera, is selected as the object of recognition. By uniformly shifting this image to the right diagonally, the Artificial Family of Images (AFI) $F_0=\{i_{01}, i_{02}, \dots, i_{06}\}$ was formed, which is shown in fig. 1.

The F_0 family is considered as an information base for conducting a computational experiment using two recognition methods based on the Fourier transform (FT) (Hindarto et al., 2024) and continuous wavelet transform (CWT) (Saraswat, 2024; Zhao et al., 2009). The processing of images from the F_0 family is carried out for three RGB models of color interpretation in shades of gray: Average, Luminosity and the proposed one under the experimental name Separate. Further, the comparison of the RGB models is carried out using the numerical criteria for evaluating recognition methods formulated and empirically substantiated in works (Kerimov, 2022; Kerimov, 2024) and (Rzayev, Kerimov et al. 2024), using the example of the AFI.

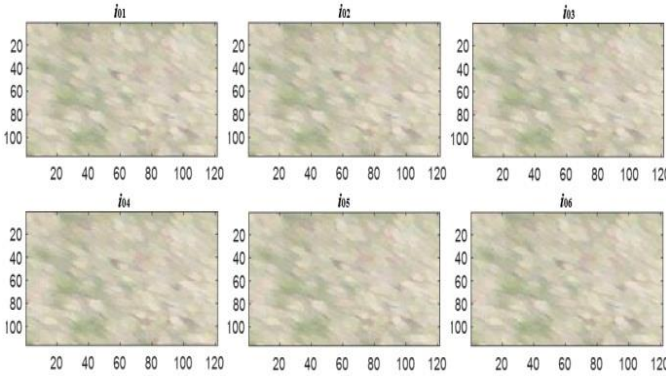


Fig. 1. The artificial family of images $F_0=\{i_{01}, i_{02}, \dots, i_{06}\}$

Assuming MV as the mean value; $D_t^\delta(s_k, s_j)$ as the Euclidean distance between two one-dimensional signals s_k and s_j ($k, j=1 \div n$) from the family $F=\{s_1, s_2, \dots, s_n\}$, where $t=1, 2, \dots$ is the ordinal number of the recognition method, these criteria are formulated as follows.

Uniformity (C_1). The distance to the standard s_1 from the signal s_k ($k=2 \div n$) increases uniformly as it is shifted. The numerical interpretation of this criterion is formulated as

$$MCV1_t^\delta = \max\{[MV(CV1_t^\delta) - CV1_t^\delta(j)]\}, \quad (1)$$

where $CV1_t^\delta(j) = [D_t^\delta(s_1, s_{j+1}) - D_t^\delta(s_1, s_j)]/\Delta\tau$ ($j=2 \div n$).

Symmetry (C_2). The distances from the signal $s_j \in F$ ($j=2 \div n-1$) to the signal on the right and to the signal on the left must be approximately equal, which predetermines the relative symmetry of the signals. The numerical interpretation of this criterion is formulated as

$$MCV2_t^\delta = \max\{[MV(CV2_t^\delta) - CV2_t^\delta(j)]\}, \quad (2)$$

where $CV2_t^\delta(j) = D_t^\delta(s_j, s_{j+1})/D_t^\delta(s_{j-1}, s_j)$ ($j=2 \div n-1$).

Operating speed (C_3). As the signals $s_j \in F$ ($j=2 \div n$) approach the standard s_1 , the rate of convergence of the values of the corresponding distances increases. The rate of convergence of the distance values is understood as $CV3_t^\delta(j) = |D_t^\delta(s_1, s_j) - D_t^\delta(s_1, s_{j+1})|/D_t^\delta(s_1, s_{j+1})$ ($j=1 \div n$). Then, criterion is formulated as

$$MCV3_t^\delta = \min\{CV3_t^\delta(j)\} \quad (j=1 \div n) \quad (3)$$

3.1. Problem definition

Color detection is an innovative computer vision technology that finds application in various fields, including the tasks of recognizing the Earth's surface to ensure the autopiloting of unmanned aerial vehicles. In particular, this technology helps multicopters recognize and interpret colors to track piloting routes and make decisions in cases of disconnection from the GPS-signal. Using the example of the selected image of the Earth's surface, it is necessary to develop an image recognition algorithm that takes into account existing methods of interpreting color in shades of gray. In the context of the above, it is necessary to develop an original approach to interpreting color and justify it using various recognition methods.

3.2. Problem solution

Transformation of images from the F_0 family with color conversion using the Average and Luminosity methods forms the new corresponding grayscale image families $F_{x0}=\{i_{x1}, i_{x2}, \dots, i_{x6}\}$ and $F_{y0}=\{i_{y1}, i_{y2}, \dots, i_{y6}\}$. Further, these families are transformed into corresponding sets of one-dimensional signals $F_x=\{x_1, x_2, \dots, x_6\}$ and $F_y=\{y_1, y_2, \dots, y_6\}$ (fig. 2) by linearizing the grayscale images as two-dimensional signals.

The Separate method interprets color in shades of gray for each R, G, and B component separately. As a result, the family of 18 grayscale images is formed as $F_{zs}=\{R_1, R_2, \dots, R_6; G_1, G_2, \dots, G_6; B_1, B_2, \dots, B_6\}$, which after the linearization procedure is represented as the set of one-dimensional signals $F_z=\{r_1, r_2, \dots, r_6; g_1, g_2, \dots, g_6; b_1, b_2, \dots, b_6\}$.

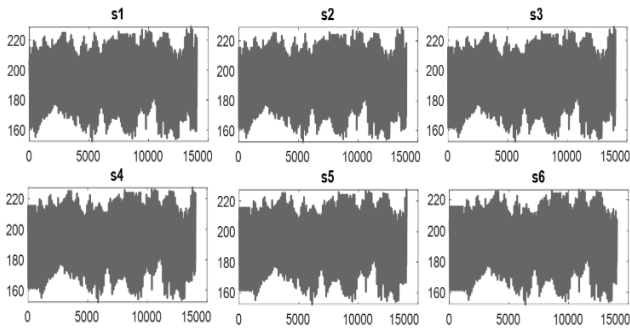


Fig. 2. The set of one-dimensional signals

This set is reflected in fig. 3, where $s_kRGB1=r_k$, $s_kRGB2=g_k$, $s_kRGB3=b_k$, ($k=1\div 6$).

Further, based on the F_x , F_y , and F_z families, an empirical analysis of three approaches to interpreting the RGB-model of the image color gamut is carried out.

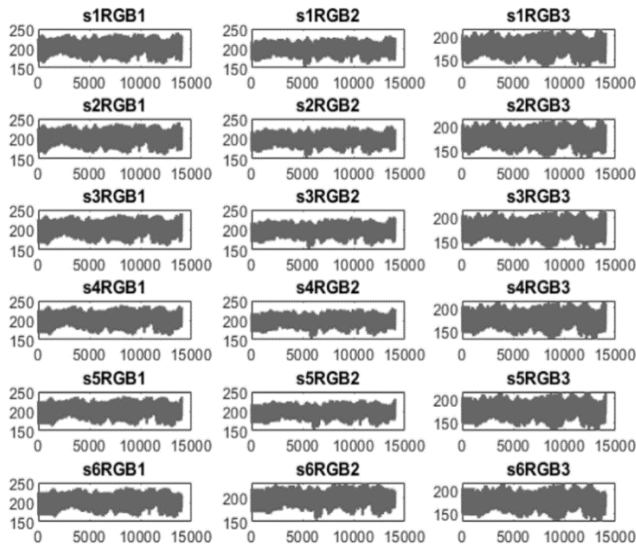


Fig. 3. The family of one-dimensional signals F_z

3.3. Image recognition using RGB models for grayscale color interpretation

The FT and CWT based recognition methods are considered. In particular, Tables 1, 2 and 3 present the results of pairwise comparison of signals from the families using the FT. In this case, the Euclidean metric is used as a criterion for comparing signals from the F_z family, i.e. the distance between the rgb_k and rgb_j signals ($k, j=1\div 6$) at the sample points is determined as

$$d = \sqrt{(r_k - r_j)^2 + (g_k - g_j)^2 + (b_k - b_j)^2}. \quad (4)$$

Table 1. Pairwise comparison of signals from F_x by FT

	x_1	x_2	x_3	x_4	x_5	x_6
x_1	0	7.0420	12.0148	15.5216	18.5174	20.6171
x_2	7.0420	0	9.7347	13.8323	17.1261	19.3771
x_3	12.0148	9.7347	0	9.8269	14.0904	16.7544
x_4	15.5216	13.8323	9.8269	0	10.0981	13.5699

x_5	18.5174	17.1261	14.0904	10.0981	0	9.0648
x_6	20.6171	19.3771	16.7544	13.5699	9.0648	0

Table 2. Pairwise comparison of signals from F_y by FT

	y_1	y_2	y_3	y_4	y_5	y_6
y_1	0	7.0153	11.9714	15.5384	18.6047	20.7055
y_2	7.0153	0	9.7005	13.8646	17.2314	19.4809
y_3	11.9714	9.7005	0	9.9060	14.2416	16.8939
y_4	15.5384	13.8646	9.9060	0	10.2320	13.6849
y_5	18.6047	17.2314	14.2416	10.2320	0	9.0874
y_6	20.7055	19.4809	16.8939	13.6849	9.0874	0

Table 3. Pairwise comparison of signals from F_z by FT

	rgb_1	rgb_2	rgb_3	rgb_4	rgb_5	rgb_6
rgb_1	0	12.1979	20.8119	26.8918	32.0777	35.6974
rgb_2	12.1979	0	16.8625	23.9663	29.6680	33.5487
rgb_3	20.8119	16.8625	0	17.0305	24.4099	29.0029
rgb_4	26.8918	23.9663	17.0305	0	17.4873	23.4762
rgb_5	32.0777	29.6680	24.4099	17.4873	0	15.6628
rgb_6	35.6974	33.5487	29.0029	23.4762	15.6628	0

Following Tables 4, 5 and 6 present numerical assessments of the FT-based recognition method ($t=1$) for its compliance with criteria C_1 , C_2 and C_3 for each considered modes of color interpretation.

Table 4. Numerical evaluation FT-based recognition method for its compliance with criterion C_1

RGB model	$CV1_1^\delta(2)$	$CV1_1^\delta(3)$	$CV1_1^\delta(4)$	$CV1_1^\delta(5)$	$MCV1_1^\delta$
Average	0.7061	0.2919	0.1930	0.1134	0.7061
Luminosity	0.7065	0.2980	0.1973	0.1129	0.7065
Separate	0.7062	0.2921	0.1928	0.1128	0.7062

Table 5. Numerical evaluation FT-based recognition method for its compliance with criterion C_2

RGB model	$CV2_1^\delta(2)$	$CV2_1^\delta(3)$	$CV2_1^\delta(4)$	$CV2_1^\delta(5)$	$MCV2_1^\delta$
Average	0.3824	0.0095	0.0276	0.1140	0.3824
Luminosity	0.3828	0.0212	0.0329	0.1260	0.3828
Separate	0.3824	0.0100	0.0268	0.1165	0.3824

Table 6. Numerical evaluation FT-based recognition method for its compliance with criterion C_3

RGB model	$CV3_1^\delta(2)$	$CV3_1^\delta(3)$	$CV3_1^\delta(4)$	$CV3_1^\delta(5)$	$MCV3_1^\delta$
Average	0.8982	0.8382	0.7741	0.5861	0.5861
Luminosity	0.8985	0.8352	0.7704	0.5860	0.5860
Separate	0.8986	0.8383	0.7739	0.5861	0.5861

The overall assessments of the recognition method using FT for its compliance with criteria C_1 , C_2 and C_3 for the considered RGB models are summarized in Table 7.

Table 7. Overall estimates of the FT-based method

RGB-model	Criterion			Total
	C_1	C_2	C_3	
Average	0.7061	0.3824	0.5861	2.7946
Luminosity	0.7065	0.3828	0.5860	2.7957
Separate	0.7062	0.3824	0.5861	2.7947

In a similar manner, the results of the pairwise comparison of signals from the F_x , F_y , and F_z families using the CWT were obtained and are summarized in the corresponding Tables 8, 9 and 10.

Table 8. Comparison of signals from F_x by CWT

	x_1	x_2	x_3	x_4	x_5	x_6
x_1	0	7.1312	16.5840	21.1119	25.7696	29.8358
x_2	7.1312	0	15.2183	19.9766	24.8371	29.0167
x_3	16.5840	15.2183	0	13.3157	19.9064	25.1127
x_4	21.1119	19.9766	13.3157	0	14.8722	21.3826
x_5	25.7696	24.8371	19.9064	14.8722	0	15.5397
x_6	29.8358	29.0167	25.1127	21.3826	15.5397	0

Table 9. Comparison of signals from F_y by CWT

	y_1	y_2	y_3	y_4	y_5	y_6
y_1	0	6.1981	14.0124	17.7900	21.5700	24.8451
y_2	6.1981	0	13.3460	17.1312	21.0356	24.3434
y_3	14.0124	13.3460	0	11.1964	16.5145	20.7490
y_4	17.7900	17.1312	11.1964	0	12.2572	17.5433
y_5	21.5700	21.0356	16.5145	12.2572	0	12.8043
y_6	24.8451	24.3434	20.7490	17.5433	12.8043	0

Table 10. Comparison of signals from F_z by CWT

	rgb_1	rgb_2	rgb_3	rgb_4	rgb_5	rgb_6
rgb_1	0	14.4215	30.4457	39.1328	48.0167	55.9613
rgb_2	14.4215	0	27.6007	36.8056	46.1270	54.3210
rgb_3	30.4457	27.6007	0	25.1749	37.6689	47.8158
rgb_4	39.1328	36.8056	25.1749	0	28.1628	40.8412
rgb_5	48.0167	46.1270	37.6689	28.1628	0	29.9479
rgb_6	55.9613	54.3210	47.8158	40.8412	29.9479	0

Following Tables 11, 12 and 13 present numerical assessments of the CWT-based recognition method ($t=2$) for its compliance with criteria C_1 , C_2 and C_3 for each considered modes of color interpretation.

Table 11. Numerical evaluation CWT-based recognition method for its compliance with criterion C_1

RGB model	$CV1_2^{\delta}(2)$	$CV1_2^{\delta}(3)$	$CV1_2^{\delta}(4)$	$CV1_2^{\delta}(5)$	$MCV1_2^{\delta}$
Average	1.3256	0.2730	0.2206	0.1578	1.3256
Luminosity	1.2608	0.2696	0.2125	0.1518	1.2608
Separate	1.1111	0.2853	0.2270	0.1655	1.1111

Table 12. Numerical evaluation CWT-based recognition method for its compliance with criterion C_2

RGB model	$CV2_2^{\delta}(2)$	$CV2_2^{\delta}(3)$	$CV2_2^{\delta}(4)$	$CV2_2^{\delta}(5)$	$MCV2_2^{\delta}$
Average	1.1340	0.1429	0.1169	0.0449	1.1340
Luminosity	1.1533	0.1920	0.0947	0.0446	1.1533
Separate	0.9139	0.0964	0.1187	0.0634	0.9139

Table 13. Numerical evaluation CWT-based recognition method for its compliance with criterion C_3

RGB model	$CV3_2^{\delta}(2)$	$CV3_2^{\delta}(3)$	$CV3_2^{\delta}(4)$	$CV3_2^{\delta}(5)$	$MCV3_2^{\delta}$
Average	0.8637	0.8193	0.7855	0.4300	0.4300
Luminosity	0.8682	0.8248	0.7877	0.4423	0.4423
Separate	0.8580	0.8150	0.7780	0.4737	0.4737

The overall assessments of the recognition method using CWT for its compliance with criteria

C_1 , C_2 and C_3 for the considered RGB models are summarized in Table 14.

Table 14. Overall estimates of the CWT-based recognition method

RGB model	Criterion			Total
	C_1	C_2	C_3	
Average	1.3256	1.1340	0.4300	4.7851
Luminosity	1.2608	1.1533	0.4423	4.6748
Separate	1.1111	0.9139	0.4737	4.1361

4. Discussion

The obtained results of pairwise comparison of signals from the F_z family demonstrate a monotone increase in comparative estimates in order of increasing indices of the rgb_k ($k=2\div 6$) signals, both in the case of using the FT and CWT-based recognition method (see the 1st lines in tables 3 and 10, respectively). Such growth is natural, which is actually confirmed by analogous results obtained using the image processing by Average and Luminosity RGB-models. This statement can be considered as an indirect confirmation of the validity of the Separate RGB model.

Another, more objective verification feature of the proposed approach is the results of an empirical analysis of FT-based and CWT-based recognition methods for their compliance with criteria C_1 , C_2 and C_3 , conducted on the basis of F_x , F_y and F_z , formed by identifying recognition features using Average, Luminosity and Separate RGB models of the color gamut of the selected images. As can be seen from tables 7 and 14, the total estimates of recognition methods for criteria C_1 , C_2 and C_3 , obtained using the Separate RGB-model, are significantly lower than the corresponding estimates obtained using Average and Luminosity RGB-models. This fact can already be considered an objective argument in favor of the approach based on the interpretation of color using the Separate method.

The proposed approach to color interpretation was tested using the example of recognizing the image: image₁ of the Earth's surface recorded by a quadcopter's onboard camera during its flight. Recognition of this image was carried out by comparing it with other three images: image₂, image₃, and image₄ (fig. 4). Comparisons of these images are carried out using FT and CWT-based recognition methods using three RGB models on different color spaces limited by the corresponding fragments of images.

Example 1. Fragmentation: height 1÷116 and width 1÷121 for image₁; height 15÷300 and width

15÷300 for image₂, image₃, and image₄ (fig. 4)

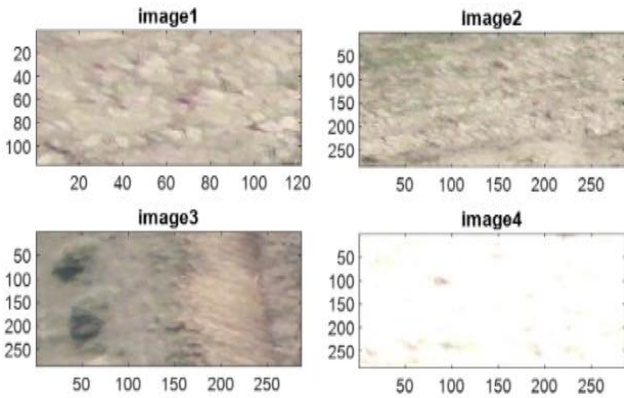


Fig. 4. Landscape images captured by the quadcopter's onboard camera

Interpreting color in grayscale using the Separate RGB model allowed us to obtain the family of 12 grayscale images, which after the linearization procedure is represented as the set of one-dimensional signals $F_z = \{s_1RGB_1, \dots, s_4RGB_1; s_1RGB_2, \dots, s_4RGB_2; s_1RGB_3, \dots, s_4RGB_3\}$ (fig. 5).

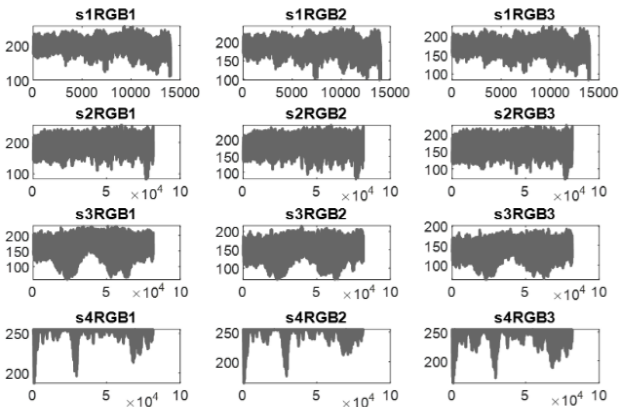


Fig. 5. The set of one-dimensional signals F_z

Pairwise comparisons of one-dimensional signals are presented in the following tables.

Table 15. FT-based pairwise comparison of signals using Average RGB-model

	x_1	x_2	x_3	x_4
x_1	0	35.3762	105.5569	170.7417
x_2	35.3762	0	99.4524	174.3680
x_3	105.5569	99.4524	0	200.7361
x_4	170.7417	174.3680	200.7361	0

Table 16. FT-based pairwise comparison of signals using Luminosity RGB-model

	y_1	y_2	y_3	y_4
y_1	0	31.0265	107.4015	168.3893
y_2	31.0265	0	102.8223	171.2238
y_3	107.4015	102.8223	0	199.7249
y_4	168.3893	171.2238	199.7249	0

Table 17. FT-based pairwise comparison of signals using Separate RGB-model

	rgb_1	rgb_2	rgb_3	rgb_4
rgb_1	0	61.2938	183.0551	295.0346
rgb_2	61.2938	0	172.4884	301.3343
rgb_3	183.0551	172.4884	0	347.2097
rgb_4	295.0346	301.3343	347.2097	0

Table 18. CWT-based pairwise comparison of signals using Average RGB-model

	x_1	x_2	x_3	x_4
x_1	0	75.7562	132.7681	92.3287
x_2	75.7562	0	109.4504	115.4042
x_3	132.7681	109.4504	0	155.0692
x_4	92.3287	115.4042	155.0692	0

Table 19. CWT-based pairwise comparison of signals using Luminosity RGB-model

	y_1	y_2	y_3	y_4
y_1	0	73.1345	134.9654	96.4941
y_2	73.1345	0	113.6547	116.3685
y_3	134.9654	113.6547	0	158.6695
y_4	96.4941	116.3685	158.6695	0

Table 20. CWT-based pairwise comparison of signals using Separate RGB-model

	rgb_1	rgb_2	rgb_3	rgb_4
rgb_1	0	132.6496	232.5855	160.1340
rgb_2	132.6496	0	192.1787	200.8260
rgb_3	232.5855	192.1787	0	270.7711
rgb_4	160.1340	200.8260	270.7711	0

Example 2. Fragmentation: height 1÷116 and width 1÷121 for image₁; height 1÷400 and width 1÷400 for image₂, image₃, and image₄ (fig. 6)

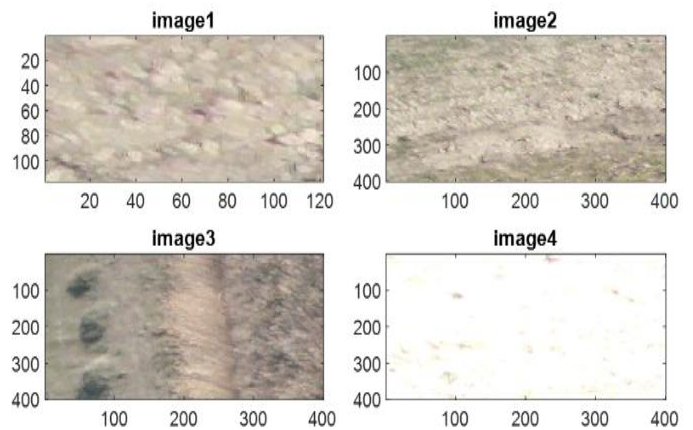


Fig. 6. Landscape images captured by the quadcopter's onboard camera

Interpreting color in grayscale using the Separate RGB model allowed us to obtain the family of 12 grayscale images, which after the linearization procedure is represented as the set of one-dimensional signals $F_z = \{s_1RGB_1, \dots, s_4RGB_1; s_1RGB_2, \dots, s_4RGB_2; s_1RGB_3, \dots, s_4RGB_3\}$ (fig. 7).

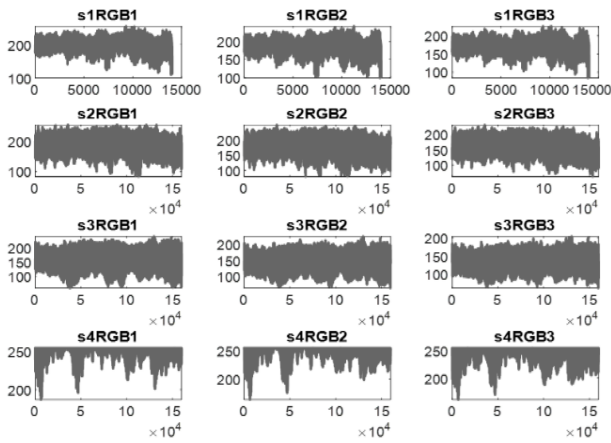


Fig. 7. The set of one-dimensional signals F_z

Pairwise comparisons of one-dimensional signals are presented in the following tables.

Table 21. FT-based pairwise comparison of signals using Average RGB-model

	x_1	x_2	x_3	x_4
x_1	0	54.6880	110.9504	170.4593
x_2	54.6880	0	96.5361	179.0172
x_3	110.9504	96.5361	0	203.3873
x_4	170.4593	179.0172	203.3873	0

Table 22. FT-based pairwise comparison of signals using Luminosity RGB Model

	y_1	y_2	y_3	y_4
y_1	0	52.3551	113.0365	168.1989
y_2	52.3551	0	100.1808	176.1588
y_3	113.0365	100.1808	0	202.6527
y_4	168.1989	176.1588	202.6527	0

Table 23. FT-based pairwise comparison of signals using Separate RGB-model

	rgb_1	rgb_2	rgb_3	rgb_4
rgb_1	0	94.6200	192.4604	294.5466
rgb_2	94.6200	0	167.5949	309.3714
rgb_3	192.4604	167.5949	0	351.8504
rgb_4	294.5466	309.3714	351.8504	0

Table 24. CWT-based pairwise comparison of signals using Average RGB-model

	x_1	x_2	x_3	x_4
x_1	0	65.1833	127.2126	93.7979
x_2	65.1833	0	109.8486	112.0478
x_3	127.2126	109.8486	0	152.8122
x_4	93.7979	112.0478	152.8122	0

Table 25. CWT-based pairwise comparison of signals using Luminosity RGB-model

	y_1	y_2	y_3	y_4
y_1	0	62.6525	129.5583	98.3019
y_2	62.6525	0	113.8753	114.1139
y_3	129.5583	113.8753	0	156.8960
y_4	98.3019	114.1139	156.8960	0

Table 26. CWT-based pairwise comparison of signals using Separate RGB-model

	rgb_1	rgb_2	rgb_3	rgb_4
rgb_1	0	115.6780	223.0530	162.3340
rgb_2	115.6780	0	192.1046	195.4432
rgb_3	223.0530	192.1046	0	266.6787
rgb_4	162.3340	195.4432	266.6787	0

The calculations presented have shown the validity of the above assertions regarding the verification of the proposed Separate RGB-model.

4. Conclusion

This study addressed the problem of color interpretation in image processing for onboard vision systems operating under constrained computational conditions. A novel approach to grayscale color interpretation based on separate processing of RGB components was proposed and systematically evaluated in comparison with conventional Average and Luminosity methods.

The experimental framework was built on the analysis of artificial families of images and real landscape images acquired by a quadcopter’s onboard camera. After image linearization, recognition performance was assessed using two well-established signal processing techniques: Fourier transform-based and continuous wavelet transform-based recognition methods. The evaluation relied on a set of quantitative criteria characterizing uniformity, symmetry, and operating speed of recognition.

The results of extensive computational experiments demonstrate that the proposed Separate RGB interpretation approach consistently ensures more stable and informative recognition characteristics. In particular, lower total estimates for the defined criteria indicate better compliance with the expected structural properties of recognition signals, confirming the adequacy and robustness of the proposed method. These results were reproducible across different recognition methods (FT and CWT) and image fragmentations, which strengthens the validity of the conclusions.

The proposed approach offers low computational complexity, high processing speed, and ease of implementation, making it well suited for real-time onboard vision systems such as those used in unmanned aerial vehicles. Overall, the presented results confirm that separate color component interpretation expands the algorithmic base of color recognition and represents a promising direction for further development of

efficient and reliable image processing methods in practical computer vision applications.

Some aspects of system analysis, considered by R.R. Rzayev in (Rzayev, 2012; Rzayev, 2016), provided invaluable support in writing this article.

Acknowledgements

The author expresses their gratitude to Dr. of Technical Sciences, Professor Ramin Rzayev for his scientific assistance in writing this article.

References

- Afifi, M., Price, B., Cohen, S., and Brown, M. S. (2019). When color constancy goes wrong: correcting improperly white-balanced images, CVPR 2019. DOI:10.1109/CVPR.2019.00163
- Barron, J. T. (2015). Convolutional color constancy. Proceedings of the IEEE International Conference on Computer Vision (ICCV), pp. 379–387
- Batchelor, B.G. "Colour Recognition." In Machine Vision Handbook. Springer London, 2012. http://dx.doi.org/10.1007/978-1-84996-169-1_16.
- Bayraktar, R., Batur A.A., and Kadir S.B. "Colour recognition using colour histogram feature extraction and K-nearest neighbour classifier." New Trends and Issues Proceedings on Advances in Pure and Applied Sciences, no. 12 (April 30, 2020): 08–14. <http://dx.doi.org/10.18844/gjpaas.v0i12.4981>.
- Chatoux, H., Noël R., and Bruno M. "Colour key-point detection." London Imaging Meeting 2020, no. 1 (2020): 114–18. <http://dx.doi.org/10.2352/issn.2694-118x.2020.lim-02>.
- Gijsenij, A., Lu, R., and Gevers, Th. (2012). Color constancy for multiple light sources, IEEE Transactions on Image Processing, 21(2): 697–707
- Haindl, M., and Stanislav, M. "Colour Texture Segmentation Using Modelling Approach." In Pattern Recognition and Image Analysis. Springer Berlin Heidelberg, 2005. http://dx.doi.org/10.1007/11552499_54.
- Henriques, M., Duarte V., Paulo G. and Rui M. "Fractional-Order Colour Image Processing." Mathematics 9, no. 5 (2021): 457. <http://dx.doi.org/10.3390/math9050457>.
- Hindarto, H., Anshory, I., Efiyanti, A. (2024). Feature extraction of heart signals using fast Fourier transform. <https://jurnal.unej.ac.id/index.php/prosiding/article/view/4187>.
- John, D.C. "Three Algorithms for Converting Color to Grayscale". <https://www.johndcook.com/blog/2009/08/24/algorithms-convert-color-grayscale/> (accessed May 21, 2025)
- Karaimer, H.C. and Brown, M.S. (2018). Improving color reproduction accuracy on cameras (CVPR 2018).
- Kerimov, A.B. (2022). Accuracy comparison of signal recognition methods on the example of a family of successively horizontally displaced curves. Informatics and Control Problems, 42(2), 80–91.
- Kerimov, A.B. (2024). An Algorithm the Sequence of Artificial Symmetric Signals for Comparison and Creating New Methods", Problems of Information Society, 15(2), 24-29.
- Muttayane, A. "Towards Colour Imaging with the Image Ranger." The University of Waikato, 2006. <http://hdl.handle.net/10289/2388>.
- Oliva, A., and Schyns, P.G. "Diagnostic Colours Influence Speeded Scene Recognition." Perception 25, no. 1_suppl (1996): 114. <http://dx.doi.org/10.1068/v96i1007>.
- Rzayev, R.R. (2012). Neuro-Fuzzy Modeling of Economic Behavior, Lambert Academic Publishing, Saarbrücken, 2012 (in Russian).
- Rzayev, R.R. (2016). Analytical Decision Support in Organizational Systems", Palmerium Academic Publishing, Saarbruchen, 2016 (in Russian).
- Rzayev, R.R., Kerimov, A.B., Garibli, U.G., Salmanov, F.M. (2024). Criteria for Assessing the Adequacy of Image Recognition Methods and Their Verification Using Examples of Artificial Series of Signals", Problems of Information Society, 15(1), pp. 10-17.
- Saraswat, S., Srivastava, G., Sachchidanand, N. (2024). Wavelet transform based feature extraction and classification of atrial fibrillation arrhythmia. <http://biomedpharmajournal.org/?p=17470>
- Wang, Hua. "Colour image representation by scalar variables." Thesis, Loughborough University, 1992. <https://dspace.lboro.ac.uk/2134/10477>.
- Zhao, M., Chai, Q., Zhang, Sh. (2009). A method of image feature extraction using wavelet. In PROCEEDINGS, International Conference on Intelligent Computing, ICIC, Emerging Intelligent Computing Technology and Applications, pp. 187–192.

How to cite: Vagif Aliyev (2026). On the issue of color interpretation in image processing by an onboard vision system. Problems of Information Society, 1, 95–102. <https://doi.org/10.25045/jpis.v17.i1.10>